

# Hybrid Laser-Assisted Mechanical Micromachining (LAMM) Process for Hard-to-Machine Materials

Ramesh Singh and Shreyes N. Melkote\*

\* *George W. Woodruff School of Mechanical Engineering, Georgia Institute of Technology, Atlanta, GA 30332-0405, USA*  
[ramesh.singh@me.gatech.edu](mailto:ramesh.singh@me.gatech.edu), [shreyes.melkote@me.gatech.edu](mailto:shreyes.melkote@me.gatech.edu)

Mechanical micro-cutting (e.g. micro-grooving, micro-milling) is emerging as a viable alternative to lithography based micromachining techniques for various applications in the fields of micro molding, biomedical devices, optics, and semiconductors. However, certain factors limit the workpiece materials that can be processed using mechanical micromachining methods. For difficult-to-machine materials such as mold and die steels and ceramics, limitations in cutting tool and stage stiffness and strength of the micro-tool are significant problems facing the successful application of mechanical micromachining methods. In addition, in microscale cutting, the effects of tool and precision motion stage deflections on part dimensional accuracy can be significant. This paper presents a novel hybrid Laser Assisted Mechanical Micromachining (LAMM) process that makes use of highly localized thermal softening of the hard material by continuous wave laser irradiation (2-35 W Yb-fiber laser, wavelength 1064 nm) in front of a miniature (100-500  $\mu\text{m}$  wide) TiAlN-coated tungsten carbide grooving tool. By suitably controlling the laser power, location, and spot size, it is possible to bring about a sufficiently large decrease in the work material strength and thereby minimize catastrophic tool failure, and lower the tool forces and deflection. Despite these advantages, the LAMM process may produce a heat affected zone (HAZ) that can result in potentially undesirable alteration of the workpiece microstructure. This paper presents the results of experimental characterization of the LAMM process for H-13 mold steel (42 HRC). Micro-grooving experiments are conducted in order to understand the influence of the laser variables (laser power, beam location with respect to tool) and cutting parameters (depth of cut, cutting speed and tool width) on the cutting and thrust forces and dimensional accuracy. The HAZ is characterized for pure laser heating. The results show that, for a given cutting condition, laser variables significantly influence the process responses. Plausible explanations for the observed trends are given.

**Keywords:** Laser assisted mechanical micromachining, micro-grooving, mold steel, heat affected zone

## 1. Introduction

There is a growing demand for devices with micro and meso scale features in optics, semiconductors and micro molding of plastics. To meet this demand, mechanical micro-cutting (e.g. micro-grooving, micro-milling) is emerging as a viable alternative to lithography based micromachining techniques. Lithography is not very suitable for creating free form three-dimensional shapes in a wide range of materials. The special equipment/environment requirements render these processes cost prohibitive [1]. In comparison, mechanical micromachining methods such as micro grooving/milling are capable of generating three-dimensional free-form features with micron level accuracy [2, 3] in a wide range of materials at reasonable cost. Despite potential advantages, practical use of mechanical micromachining is limited by the properties of the workpiece and tool materials. In particular, low tool stiffness and flexural strength limit the utility of mechanical micromachining methods, particularly for hard-to-machine materials such as mold/die steels and ceramics. At micro/meso length scales of cutting, the effect of tool and machine (e.g. motion stage) deflections due to high cutting forces on the dimensional accuracy can be significant. One way to ad-

dress this situation is to induce thermal softening in the workpiece material by using a laser source to heat the material during micro-cutting.

At the macro scale, laser assisted mechanical machining has been investigated extensively for processing hard-to-machine ceramics [4-8]. In addition, plasma-assisted milling of superalloys has been reported [9]. A two-step process comprising of mechanical milling and laser finishing has also been developed [10].

Pure laser micromachining is typically limited to ablative processes. The use of ultra-short pulsed (e.g. femto-second) UV lasers for pure laser micromachining has drawn the attention of researchers in the past few years. These laser systems have been successfully applied to micromachining of masks for lithography, MEMS, photonics, coronary stents and dental surgery [11-15]. Although ultra-short pulse laser micromachining yields fine detail, it is slower than mechanical micromachining. The typical material removal rates are of the order of 0.1  $\text{mm}^3/\text{min}$ -1  $\text{mm}^3/\text{min}$  for laser micromachining [16-17]. In contrast, for pure mechanical micromachining a material removal rate of 25  $\text{mm}^3/\text{min}$  has been reported [18].

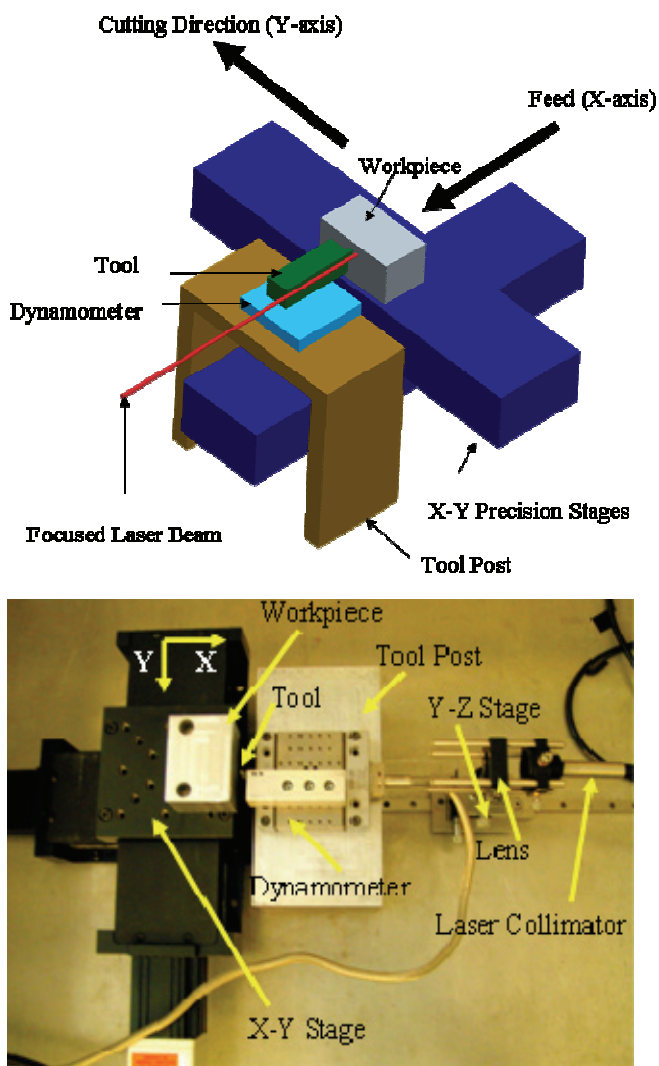


**Fig. 1** Schematic (top) and actual view (bottom) of first generation LAMM setup for micro-grooving.

Moreover, creating a sculptured surface with complex 3-D features can be difficult with these systems. A logical solution to this limitation is to employ a hybrid process that combines the beneficial aspects of laser heating and 3-D mechanical micro-cutting. Initial investigations by Singh and Melkote [19-20] have demonstrated laser softening in AISI 1018 and hardened H-13 steels. Recently, Jeon and Pfefferkorn [21] have also studied the effect of laser pre-heating on micro-end milling of metals (Al 6061-T6 and 1018 steel).

The LAMM setup (see Fig. 1) developed by Singh and Melkote [19-20] consists of a 2-35 W continuous wave Ytterbium doped fiber laser (wavelength 1064 nm) integrated with a mechanical micro grooving machine. The laser beam is focused in front of a miniature cutting tool to soften the workpiece material just ahead of the cutting tool thereby lowering the forces required to cut the material.

The present paper describes the laser assisted mechanical micromachining (LAMM) process for micro-grooving of H-13 (42 HRC), a heat treated mold steel. Cutting forces, groove depth and microstructural integrity are the experimental responses analyzed.

Note that the material removal rate in the current LAMM-based micro grooving process is  $2.5 \text{ mm}^3/\text{min}$  but once the process is well understood, it can be potentially applied to other processes such as micro-milling, where material removal rate can be up to 10 times higher.

## 2. Experimental Work

The nominal chemical composition of H-13 steel is given in Table 1. The five factors and their respective levels used in the experiment are given in Table 2. It is known from previous experiments [19] that variation in spot size in the given range does not have a significant effect on the cutting force response. Therefore, the laser spot size was kept constant at  $70 \mu\text{m}$ . The cutting tool material in this experiment was tungsten carbide (WC) coated with TiAlN. Other geometry parameters of the micro grooving tool were as follows:  $300 \mu\text{m}$  tool width, rake angle of  $0^\circ$ , back clearance angle of  $2.5^\circ$  and side clearance angle of  $5^\circ$ . Three replications were conducted for each test condition. The measured responses included the cutting (Y) force, thrust (X) force and groove profile.

**Table 1.** Nominal composition of H-13 mold steel

C	Cr	Mn	Mo	Va	Si
0.40%	5.25%	0.40%	1.35%	1.00%	1.00%

**Table 2.** Factors and their levels

Level	Depth of Cut ( $\mu\text{m}$ )	Laser Location ( $\mu\text{m}$ )	Width of cut ( $\mu\text{m}$ )	Cutting Speed (mm/min)	Laser Power (W)
0	10	100	300	10	0
1	15	200	500	50	5
2	20				10
3	25				35

Since LAMM is a heat assisted process it can induce a detrimental heat affected zone. Hence, characterization of thermal damage produced in the LAMM process is important. A continuous-wave (CW) laser set at 10 W power output and  $110 \mu\text{m}$  spot size was employed to scan the metal surface (without mechanical cutting) at 10, 50 and 100 mm/min scanning speeds. The heat affected zone caused by pure laser heating of H-13 mold steel at the given laser scanning speeds was examined using optical and metallographic techniques.

## 3. Results and Discussion

### 3.1 Characterization of the LAMM Process for H-13 Mold Steel

Figure 2 shows the cutting and thrust force data for  $20 \mu\text{m}$  depth of cut and a tool location of  $200 \mu\text{m}$  from the center of the laser spot. The mean thrust force data exhibits

a distinct decrease with increase in laser power whereas the mean cutting forces do not exhibit a prominent decrease (the one standard deviation error bars overlap in many cases). Tests are required to examine the statistical significance of the difference in the mean cutting and thrust force data.

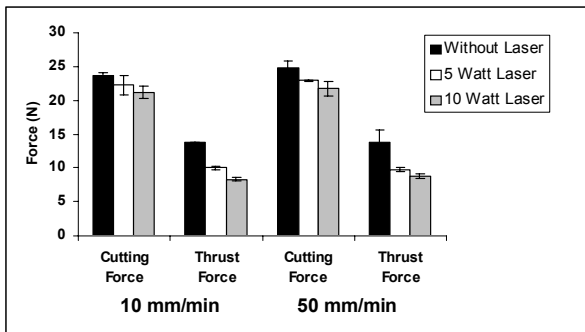


**Fig. 2** Cutting and thrust forces at 20 μm depth of cut for 300 μm tool width and tool location of 200 μm from the center of the laser spot; error bars denote one standard deviation of the data.

Paired student *t*-tests were performed to test the differences in the mean forces for the different laser power cases. It was observed that the differences in cutting force with and without laser heating are not statistically significant at 5% risk level in all the cases except for the 0 W and 10 W laser powers and 10 mm/min cutting speed. The thrust force data with and without laser heating were found to be statistically different for all four cases shown in Fig. 2 (0 W and 5 W, and 0 W and 10 W at both cutting speeds). A test of the alternate hypothesis showed that the thrust forces at 5 W and 10 W laser powers are statistically lower than the thrust force data obtained without laser heating.

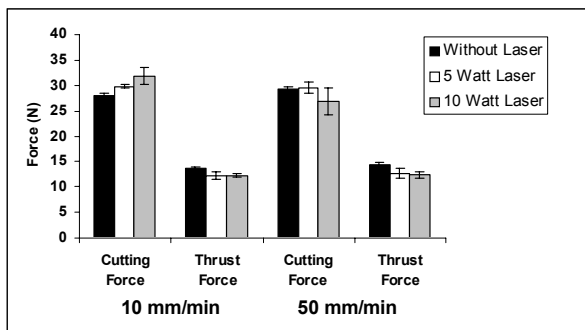


**Fig. 3** Cutting and thrust forces at 25 μm depth of cut for 300 μm tool width and tool location of 100 μm from the center of the laser spot.

Figure 3 shows the cutting and thrust force data for 25 μm depth of cut and a tool location of 100 μm from the center of the laser beam. The mean cutting force data does not exhibit a consistent trend with increase in laser power. On the other hand, the mean thrust force data shows a decrease with increase in laser power although the difference between the 5 W and 10 W cases does not appear to be significant.

Paired student *t*-tests showed that the differences in the cutting force at 0 W and 5 W, and 0 W and 10 W at 10

mm/min are statistically significant at 5% risk level. The thrust force data at 10 W and 5 W laser powers are statistically different from the thrust force data without laser heating at both speeds. The thrust force data showed no significant difference between the 5 W and 10 W laser powers.

For the cases shown in Figs. 2 and 3, the cutting force does not exhibit a significant change with increase in laser power. In contrast, the thrust force generally decreases with increase in laser power. A decrease of 40% in the mean thrust force is observed when the laser power is increased from 0 W to 10 W at 10 mm/min for 20 μm depth of cut with the laser spot located 200 μm from the tool. A decrease of 37% is observed when the speed is increased to 50 mm/min (see Fig. 2). The mean thrust force decreases by 8% and 13% at 10 mm/min and 50 mm/min, respectively, at 25 μm depth of cut and with the laser located 100 μm from the tool (see Fig. 3).

These results can be explained as follows. The LAMM setup has a finite stiffness (3 N/μm in the thrust force direction) and can deflect under the influence of forces (especially the thrust force), which in turn can affect the actual depth of cut. Since the depth of cut is of the order of a few microns, a small deflection of the machine and/or thermal expansion of the tool can change the depth of cut. Previous studies [19-20] have shown that the thermal expansion of the tool can be as high as 2.2 μm. The reduced thrust force due to laser heating causes a smaller deflection of the machine stage and results in a higher effective depth of cut than that obtained without laser heating. Additionally, thermal expansion of the tool due to laser heating yields a higher actual depth of cut. The cumulative increase in the depth of cut due to smaller machine deflection and tool thermal expansion can offset the effect of lower material strength due to thermal softening. Consequently, the measured forces may not always exhibit the expected decrease with laser heating as seen in the cutting force data at 10 mm/min in Fig. 3.

The reason that the decrease in the thrust force is more pronounced than in the cutting force is probably due to the inherently greater sensitivity of the thrust force to changes in material strength.

A white light interferometer image of the cut groove geometry is shown in Fig. 4. The difference between the perpendicular trace (shown by the double-headed arrow in Fig. 4) extracted for the pass with laser heating and superimposed on the preceding clean-up pass provides the actual depth of cut for that pass. Note that clean-up cuts are required for removing the laser marks burnt during the laser spot alignment process [20].

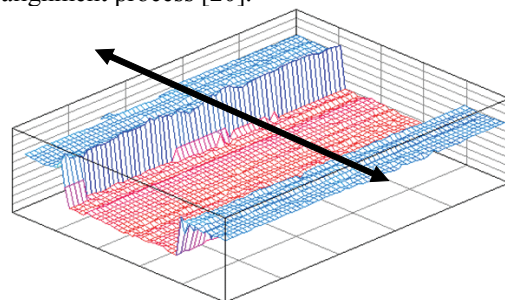
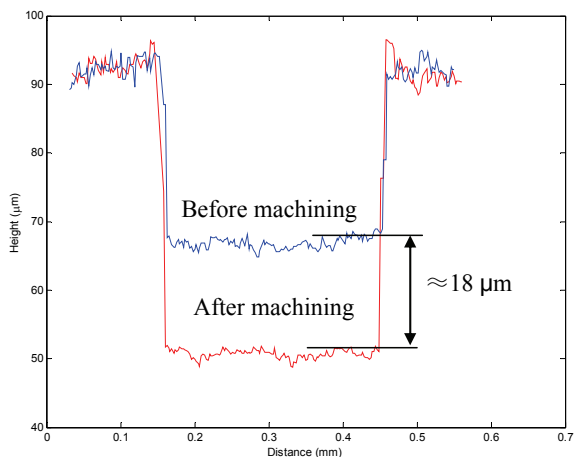
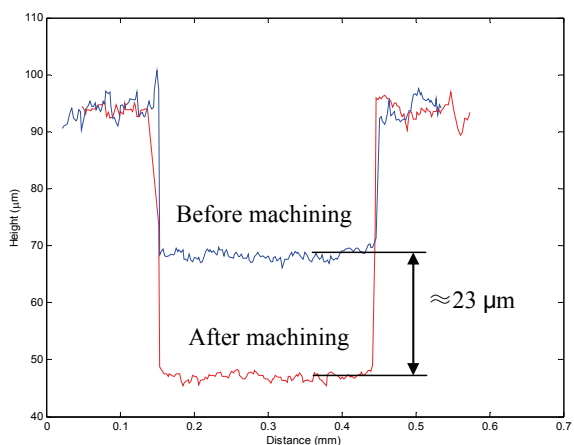


**Fig. 4** 3-D plot of a typical micro groove

Figure 5 shows the actual depth of the cut grooves for 25  $\mu\text{m}$  depth of cut, 10 W laser power, 10 mm/min cutting speed and laser beam center located 100  $\mu\text{m}$  from the tool. At 25  $\mu\text{m}$  nominal depth of cut, the dimensional accuracy of the groove depth increases significantly with laser heating.



(a) Without laser



(b) With 10 W laser

**Fig. 5** Measured depth of groove machined at 25  $\mu\text{m}$  nominal depth of cut (a) without laser heating, (b) with 10 W laser heating at 10 mm/min

The dimensional error with laser heating is 8% as compared to 30% without laser heating. It can be seen from Fig. 5 that higher actual depths of cut are observed with laser heating compared to without laser heating, which, as mentioned earlier, can be attributed to the effective increase in the depth of cut due to reduced machine deflection and tool thermal expansion. As a result, the measured depth of cut with laser heating is closer to the nominal depth of cut for the conditions investigated here.

It is expected that if the laser power is increased further the thermal softening will offset the effect of machine-tool system deflection. Figure 6 shows the cutting and thrust forces for 25  $\mu\text{m}$  nominal depth of cut and 10 mm/min cutting speed and 0 W and 35 W laser powers, respectively.

It can be seen from Fig. 6 that there is a reduction of 55% in the cutting force and 46% in thrust force for 35 W

laser power compared to no laser heating. It is clear from the results that a sufficiently high laser power can reduce the material flow stress and consequently the cutting and thrust forces

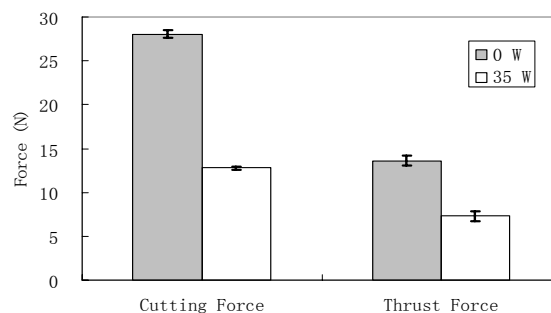
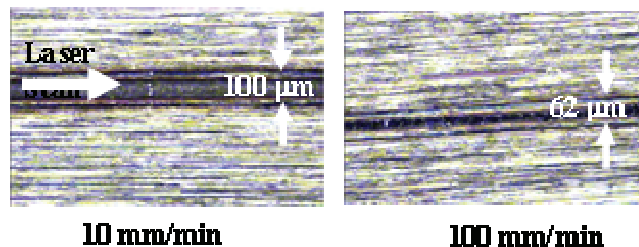


**Fig. 6** Measured cutting and thrust forces at 0 W and 35 W laser powers.

### 3.2 Microstructure of H-13 Mold Steel in LAMM Process

In order to examine the effect of laser heating on thermal damage, experiments were performed with laser heating only and with laser assisted mechanical micro grooving. Fig. 7 shows optical images of the H-13 workpiece surface scanned by the laser (without mechanical cutting) at different speeds. The heat affected area is clearly visible in each image.

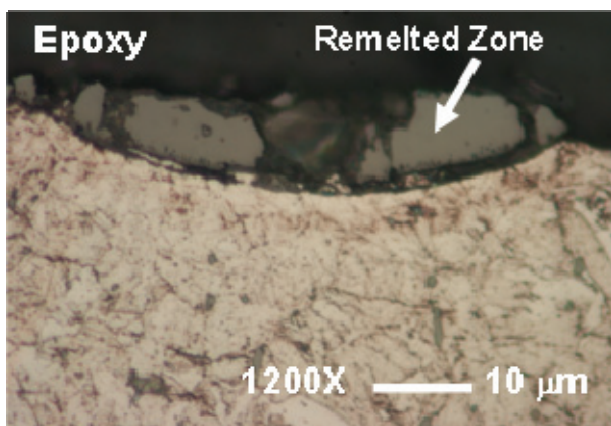
The width of the visible laser affected area is 100  $\mu\text{m}$  for 10 mm/min scan speed and it decreases to 62  $\mu\text{m}$  for 100 mm/min scan speed. It can be observed that the heat affected area is confined to smaller widths with increase in laser speed.



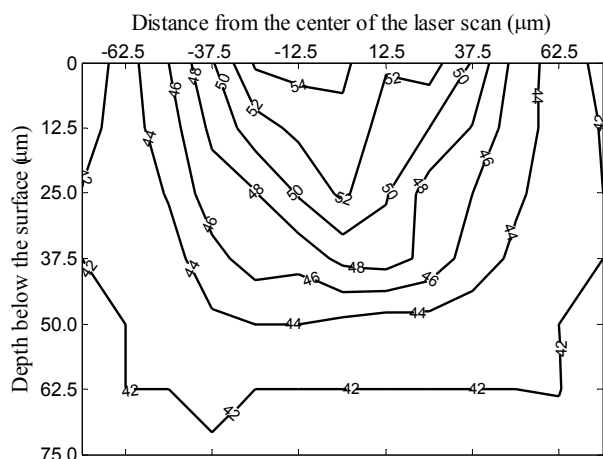
**Fig. 7** Surface morphology of H-13 steel (42 HRC) exposed to laser scans (CW, 10W, 100  $\mu\text{m}$  spot size) at 10 mm/min and 50 mm/min scanning speeds.

Figure 8 shows the optical micrograph of the cross-sectioned workpiece sample shown in Fig. 7 for 10 mm/min scanning speed. The micrograph shows the presence of a remelted zone, which is a hard brittle layer formed by solidification of the molten metal pool. The remelted zone has an uneven surface due to fracture of the brittle layer during polishing. The bulk microstructure is tempered martensite. The tempered martensite bulk may undergo hardening due to phase transformation. To ascertain the extent of the HAZ, microhardness tests were conducted at a load of 50 g and the results are shown in Fig. 9. The hardness varies from 54 HRC right below the center of the laser spot to about 44 HRC at 50  $\mu\text{m}$  below the surface. Note that the bulk hardness is 42 $\pm$ 2 HRC. The change in

hardness suggests that a phase transformation resulting in hardening may have taken place.



**Fig. 8** Micrographs of H-13 steel (42 HRC) exposed to laser scans (CW, 10W, 100  $\mu\text{m}$  spot size) at 10 mm/min scanning speeds.



**Fig. 9** Temperature and hardness contours in the cross-section of the HAZ at 10 W laser power and 10 mm/min scan speed.

The mechanism of laser hardening is well understood. The high intensity laser irradiation rapidly heats the steel surface into the austenitic region described by the critical temperatures  $A_{c1}$  and  $A_{c3}$ . For H-13 steels, austenitization starts when the temperature reaches the  $840^{\circ}\text{C}$  ( $A_{c1}$ ) and is completed at  $890^{\circ}\text{C}$  ( $A_{c3}$ ) the austenitization. The very steep temperature gradients result in rapid cooling by conduction of heat from the surface to the bulk. This causes the transformation from austenite to martensite without external quenching. This self-quenching occurs as the low temperature of the bulk provides a sufficiently large heat sink to quench the hot surface by heat conduction to the interior at a rate high enough to prevent pearlite or bainite formation at the surface, resulting in untempered martensite formation instead [22].

A 3-D transient finite element based thermal model of heating due to a moving laser beam has been presented elsewhere [23-24] to analyze the temperatures generated in the vicinity of the laser spot. That model has been validated through actual temperature measurements. Model simulations show that the temperature in the vicinity of laser spot

can be as high as  $1876^{\circ}\text{C}$  at 10 W laser power and 10 mm/min scanning speed [24]. This is much higher than the melting point of H-13 mold steel and explains the presence of the remelted zone observed in Fig. 8. Also, the simulated temperature corresponding to the transition hardness is found to be close to the  $A_{c1}$  temperature [24].

#### 4. Conclusion

This paper presented an experimental characterization of a laser-assisted mechanical micromachining process for hard-to-machine materials. The process attempts to overcome the limitations of pure mechanical micro cutting in terms of the low tool stiffness and bending strength and the geometry limitations of pure laser micromachining. The finite machine stiffness and thermal expansion of the tool can affect the actual depth of cut in micro-cutting. The study suggests that laser softening improves the dimensional accuracy of the cut grooves in H-13 mold steel by reducing the machine/stage deflection. The LAMM process may result in undesirable residual HAZ after machining. The critical temperature can be used to predict the region of HAZ. The following specific conclusions can be drawn from this study:

- Thermal softening can be induced in H-13 mold steel by laser heating and up to 40% reduction in the thrust force is observed with laser heating.
- At low laser powers, a decrease in the cutting force with laser heating is not observed for H-13 mold steel because of an increase in the actual depth of cut due to smaller stage deflection (as a result of lower thrust forces) and thermal expansion of the tool.
- The heat affected region in H-13 steel is reduced with increase in the laser scanning speed.
- Microhardness data reveal the presence of a measurable HAZ below the laser scanned surface.

#### Acknowledgments and Appendixes

The authors gratefully acknowledge the support of The Timken Company.

#### References

- [1] Tai-Ran Hsu, MEMS and microsystems design and manufacture, McGraw Hill Company, New York, 1st Edition, 2002.
- [2] T. Masuzawa, and H. K. Toneshoff, Annals of the CIRP, 46, 2, (1997), 621-628.
- [3] D. Cox, G. Newby, H. W. Park, and S. Y. Liang, IMECE, Anaheim, CA, Paper No. IMECE2004-62186 (2004), 1-6
- [4] W. Konig, and A. K. Zaboklicki, International Conference on Machining of Advanced Materials, NIST special Publication, 847, (1993), 455-463.
- [5] S. Lei, and Y. C. Shin, Journal of Manufacturing Science and Engineering, 123, (2001), 639-646.
- [6] J. C. Rozzi, F. E. Pfefferkorn, and Y. C. Shin, Journal of Manufacturing Science and Engineering, 122, (2000), 666-670.

- [7] P. A. Rebro, Y. C. Shin, and F. P. Incropera, *Journal of Manufacturing Science and Engineering*, 124, (2002), 875-885.
- [8] F. E. Pfefferkorn, Y. C. Shin, and F. P. Incropera, *Journal of Manufacturing Science and Engineering*, 126, (2004), 42-51.
- [9] L. N. Lo'pez de Lacalle, J. A. Sa'nchez, A. Lamikiz , and A. Celaya, *Journal of Manufacturing Science and Engineering*, 126, (2004), 274-285.
- [10] A. Kaldos, and H. J. Pieper, *Journal of Materials Processing Technology* 155-56, (2004), 1815-1820.
- [11] C. Momma, U. Knop, U., and S. Nolte, *Progress in Biomedical Research*, 4, 1, (1999), 39-44.
- [12] J. Servin, T. Bauer, and C. Fallnich, *Applied Surface Science*, 197, (2002), 737-740.
- [13] I. V. Hertel, *Proceedings of the SPIE*, 4088, (2000), 17-24.
- [14] M. R. Kasaai, V. Kacham, F. Theberge, and S. L. Chin, *Journal of Non-Crystalline Solids*, 319, (2003), 129-135.
- [15] F. Théberge, and S. L. Chin, *Applied Physics A*, 80, (2005), 1505-1510.
- [16] D. Gómez, I. Goenaga, I. Lizuain, and M. Ozaita, *Optical Engineering*, 44, 5, (2005), 1105-1113.
- [17] G. Dumitru, V. Romano, H. P. Weber, M. Sentis, J. Hermann, S. Bruneau, W. Marine, H. Haefke, and Y. Gerbig, *Applied Surface Science*, 208, (2003), 181-188.
- [18] X. Liu, M. B.G. Jun, R. E. Devor, and S. G. Kapoor, *Proceedings of IMECE*, Anaheim, CA, IMECE2004-62416, (2004), 1-10.
- [19] R. Singh, and S. N. Melkote, 2<sup>nd</sup> JSME/ ASME International Conference on Materials and Processing, Seattle, WA, USA, (2005), 1-6.
- [20] R. Singh, and S. N. Melkote, *Proceedings of IMECE 2005: ASME International Mechanical Engineering Congress and Exposition*, Orlando, Florida, USA, (2005), 1-8.
- [21] Y. Jeon, and F. Pfefferkorn, *Proceedings of IMECE 2005 ASME International Mechanical Engineering Congress and Exposition*, Orlando, Florida, USA, (2005), 1-10
- [22] E. Kennedy, G. Byrne, and D.N. Collins, *Journal of Materials Processing Technology*, 155-156, (2004), 1855-1860.
- [23] R. Singh, M. J. Alberts, and S. N. Melkote, *Proceedings of the 1<sup>st</sup> International Conference on Micromanufacturing*, Urbana, IL, (2006), 1-6.
- [24] R. Singh, M. J. Alberts, and S. N. Melkote, submitted to *Material Science and Engineering A*.

(Received: May 16, 2006, Accepted: June 7, 2007)